

Copy No. 155

RESTRICTED

RM No. L8D01

NACA RM No. L8D01

CLASSIFICATION CHANGED

CLASSIFICATION CANCELLED

To

NACA

By authority of *Dr. J. H. Doolittle - 690* Date *DEC 28 1951*

RESEARCH MEMORANDUM

AERODYNAMIC CHARACTERISTICS OF A TWO-BLADE

NACA 10-(3)(12)-03 PROPELLER

By

W. H. Gray and A. E. Allis

Langley Aeronautical Laboratory
Langley Field, Va.

CLASSIFIED DOCUMENT

This document contains classified information affecting the National Defense of the United States within the meaning of the Espionage Act, USC 50:31 and 32. Its transmission or the revelation of its contents in any manner to an unauthorized person is prohibited by law. Information so classified may be imparted only to persons in the military and naval services of the United States, appropriate civilian officers and employees of the Federal Government who have a legitimate interest therein, and to United States citizens of known loyalty and discretion who of necessity must be informed thereof.

NATIONAL ADVISORY COMMITTEE
FOR AERONAUTICS

WASHINGTON

August 30, 1948

RESTRICTED

CLASSIFICATION CANCELLED

NATIONAL ADVISORY COMMITTEE FOR AERONAUTICS

RESEARCH MEMORANDUM

AERODYNAMIC CHARACTERISTICS OF A TWO-BLADE

NACA 10-(3)(12)-03 PROPELLER

By W. H. Gray and A. E. Allis

SUMMARY

Full-scale tests of the NACA 10-(3)(12)-03 propeller have been conducted in the Langley 16-foot high-speed tunnel. The propeller was tested at blade angles from 20° to 55° on a 2000-horsepower dynamometer through as great an advance-ratio range as the equipment permitted, from about 0.60 to 3.6.

A maximum efficiency of 0.91 was attained at a constant rotational speed of 1140 revolutions per minute. Peak efficiency, at a blade angle of 45° , was decreased 26 percent by a helical tip Mach number increase from 0.81 to 1.10.

INTRODUCTION

A series of blades were designed several years ago by the NACA for the purpose of conducting a systematic investigation of the variables involved in propeller design. The variables to be investigated were camber or design lift coefficient, solidity, airfoil section, and blade-thickness ratio. These blades were designed employing the best information then available, and for each different design the optimum efficiency was to be obtained at a blade angle of 45° at the 0.7-radius station. The particular blade design, the tests of which are described in the present paper, was one necessary to the investigation of the effect of differences in blade-thickness ratios.

TESTS

Scope

The scope of the tests was dictated by the power and speed limitations of both the wind tunnel and the dynamometer. These tests were conducted at constant values of propeller rotational speed, through a range of blade angles from 20° to 55° , the tunnel speed being varied

to suit the requirements of each test. In order to extend the range of tip speeds for a few tests at the design blade angle of 45° , the tunnel speed was fixed at predetermined values, and the propeller speed varied to include as much as possible of the propeller operating regime from peak efficiency to zero torque. A chart of the program is given as table I of this paper.

Apparatus

Dynamometer. - The tests were conducted in the Langley 16-foot high-speed tunnel with the 2000-horsepower propeller dynamometer and related equipment described in reference 1.

Blades. - The configuration of the blades tested was a two-blade propeller having a diameter of 10.05 feet. The propeller blade designation was NACA 10-(3)(12)-03, signifying blades designed for use on a propeller with a nominal diameter of 10 feet and having the following characteristics at the 0.7-radius station: a section design lift coefficient of 0.3, a section thickness-chord ratio of 12 percent, and a blade solidity of 3 percent. Solidity is defined as the ratio of the blade chord to the circumference at any specified radius. The blade-form curves for the NACA 10-(3)(12)-03 propeller design are presented in figure 1.

Reduction of Data

The values of the thrust coefficient presented are based on corrected values of thrust forces. Corrections were necessary to cancel the effects of spinner forces, spinner fairing juncture pressures, and wind-tunnel-wall interference. A detailed description of the measurements and methods necessary to the reduction of data to propeller forces only may be found in reference 1.

The test results are presented in the form of the usual thrust and power coefficients and propeller efficiency. The symbols and definitions used are as follows:

b	blade chord, feet
c_{l_d}	design section lift coefficient
C_P	power coefficient $(P/\rho n^3 D^5)$
C_T	thrust coefficient $(T/\rho n^2 D^4)$
D	propeller diameter, 10.05 feet
h	blade section maximum thickness, feet
J	advance ratio (V/nD)

M	air-stream Mach number
M_t	helical tip Mach number $\left(M \sqrt{1 + \left(\frac{T}{J} \right)^2} \right)$
n	propeller rotational speed, rps
N	propeller rotational speed, rpm
P	power absorbed by propeller, foot-pounds per second
r	radius to blade element, feet
R	propeller tip radius, feet
T	propeller thrust, pounds
V	velocity of advance, feet per second
β	blade angle, degrees
η	propeller efficiency $\left(\frac{C_T}{C_P} J \right)$
η_i	induced efficiency
η_o	profile efficiency
ρ	mass density of air in free stream, slugs per cubic foot

RESULTS

The aerodynamic results are presented as plots of thrust and power coefficients and efficiency in figures 2 to 8. In table I reference may be made to the figure numbers.

Figure 9 shows the variation of envelope efficiency for five different test rotational speeds through an advance-ratio range from 0.65 to 3.1. Envelope efficiencies of 0.90 or more were attained at all speeds from 1140 through 1600 rpm. The range of advance ratios for which the envelope efficiency was 0.90 or greater at 1140 rpm extended from $J = 1.34$ to $J = 2.67$. The maximum efficiency attained was 0.913 at 1140 rpm and at $J = 2.40$. The efficiency envelopes for the higher rotational speeds, 2000 and 2160 rpm, are much lower than the envelopes for the lower rotational speeds. At a constant rotational speed of 2160 rpm a maximum efficiency of 0.727 was attained at an advance ratio of 1.10.

Propeller efficiency losses may be separated into induced losses and profile-drag losses. The induced efficiency, the efficiency assuming only induced losses, has been calculated from the charts of

reference 2, using values of power coefficient and advance ratio obtained at a constant rotational speed of 1350 rpm. The induced efficiency envelope for this rotational speed is shown in figure 9. The profile loss for the design condition may be determined by making the assumption that $\eta_o = \eta_i$. This assumption may be shown to be justified if the design condition insures minimum induced power loss for the particular power loading at that condition. Therefore, since

$$\eta = \eta_o \eta_i$$

then

$$\eta = \eta_i^2$$

At the design blade angle of 45° at 1350 rpm, the point of tangency of the efficiency curve with the efficiency envelope is at $J = 2.0$. The value of η_i for this condition from reference 2 is 0.950 which gives a value of η_i^2 , or theoretical propeller efficiency, of 0.903. For this same advance ratio the efficiency as obtained from test data is 0.904.

The effects of compressibility on peak efficiency for a fixed blade angle of 45° are shown in figure 10. At tip Mach numbers beyond 0.810 the adverse effects of compressibility become evident as the peak efficiency drops rapidly. For a helical tip Mach number of 1.1 the peak efficiency is only 0.640 as compared to 0.900 at a helical tip Mach number of 0.810.

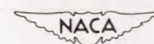
Langley Aeronautical Laboratory
National Advisory Committee for Aeronautics
Langley Field, Va.

REFERENCES

1. Corson, Blake W., Jr., and Maynard, Julian D.: The NACA 2000-Horsepower Propeller Dynamometer and Tests at High Speed of an NACA 10-(3)(08)-03 Two-Blade Propeller. NACA RM No. L7L29, 1948.
2. Crigler, John L., and Talkin, Herbert W.: Charts for Determining Propeller Efficiency. NACA ACR No. L4I29, 1944.

TABLE I

Figure	Tunnel speed	Propeller speed (rpm)	Blade angle, β , degrees at 0.75R							
				25	30	35	40	45	50	55
2	Vary	1140								
3	Vary	1350	20	25	30	35	40	45	50	
4	Vary	1500						45		
5	Vary	1600	20	25	30	35	40	45		
6	Vary	2000	20	25	30	35				
7	Vary	2160	20	25	30					
8(a)	M = 0.56	Vary						45		
8(b)	M = 0.58	Vary						45		
8(c)	M = 0.60	Vary						45		



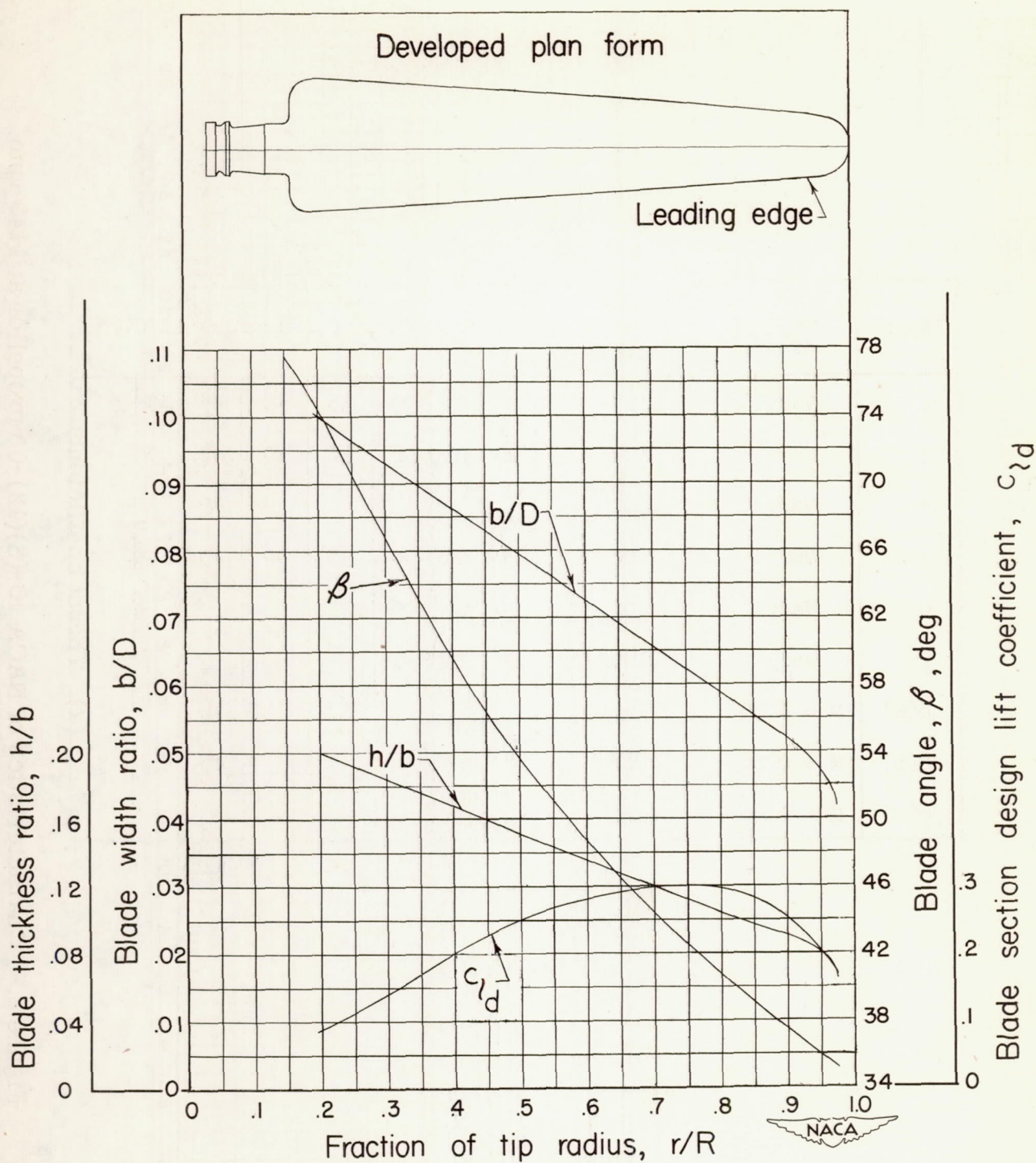
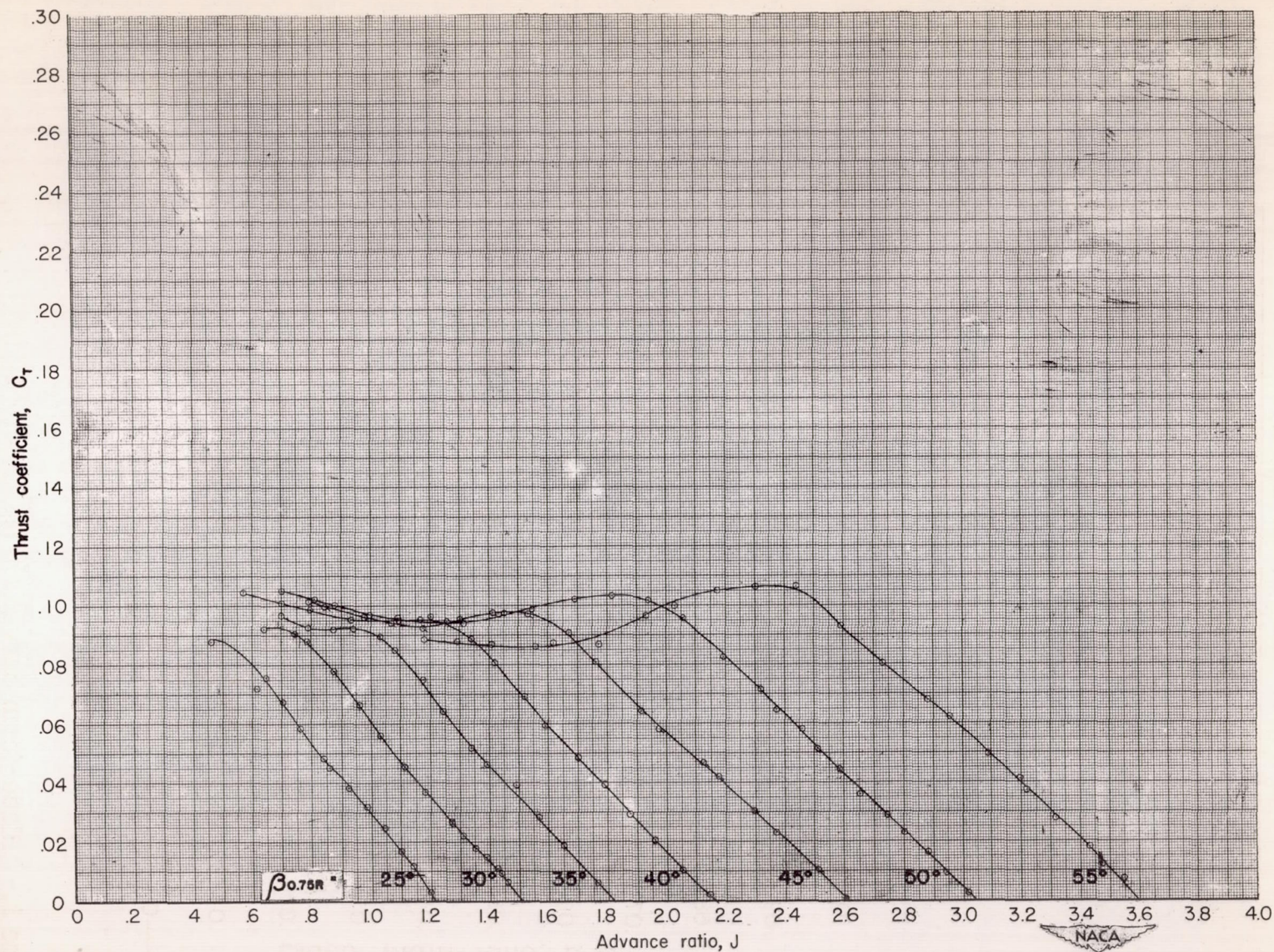
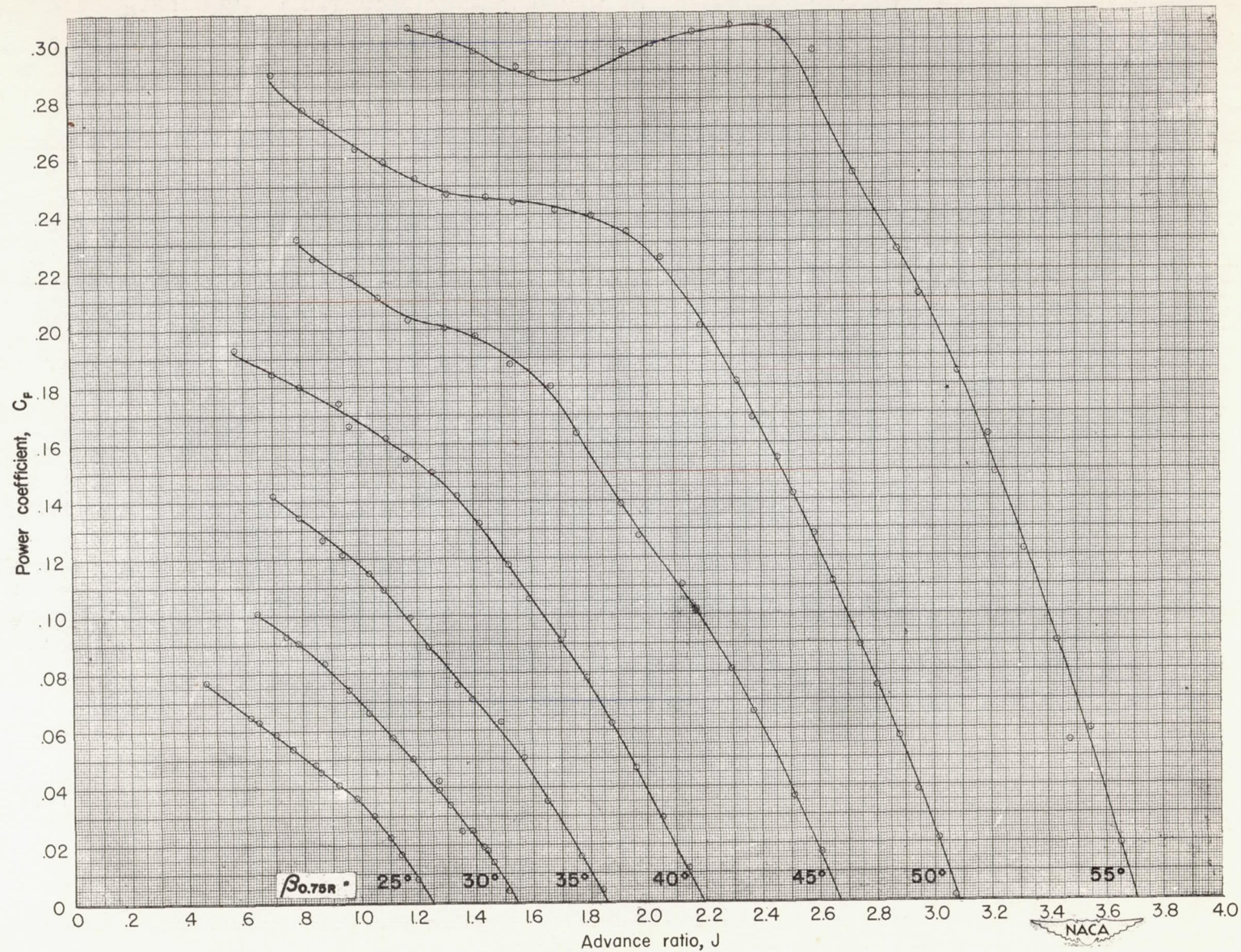


Figure 1.- Blade-form curves for NACA 10-(3)(12)-03 propeller.



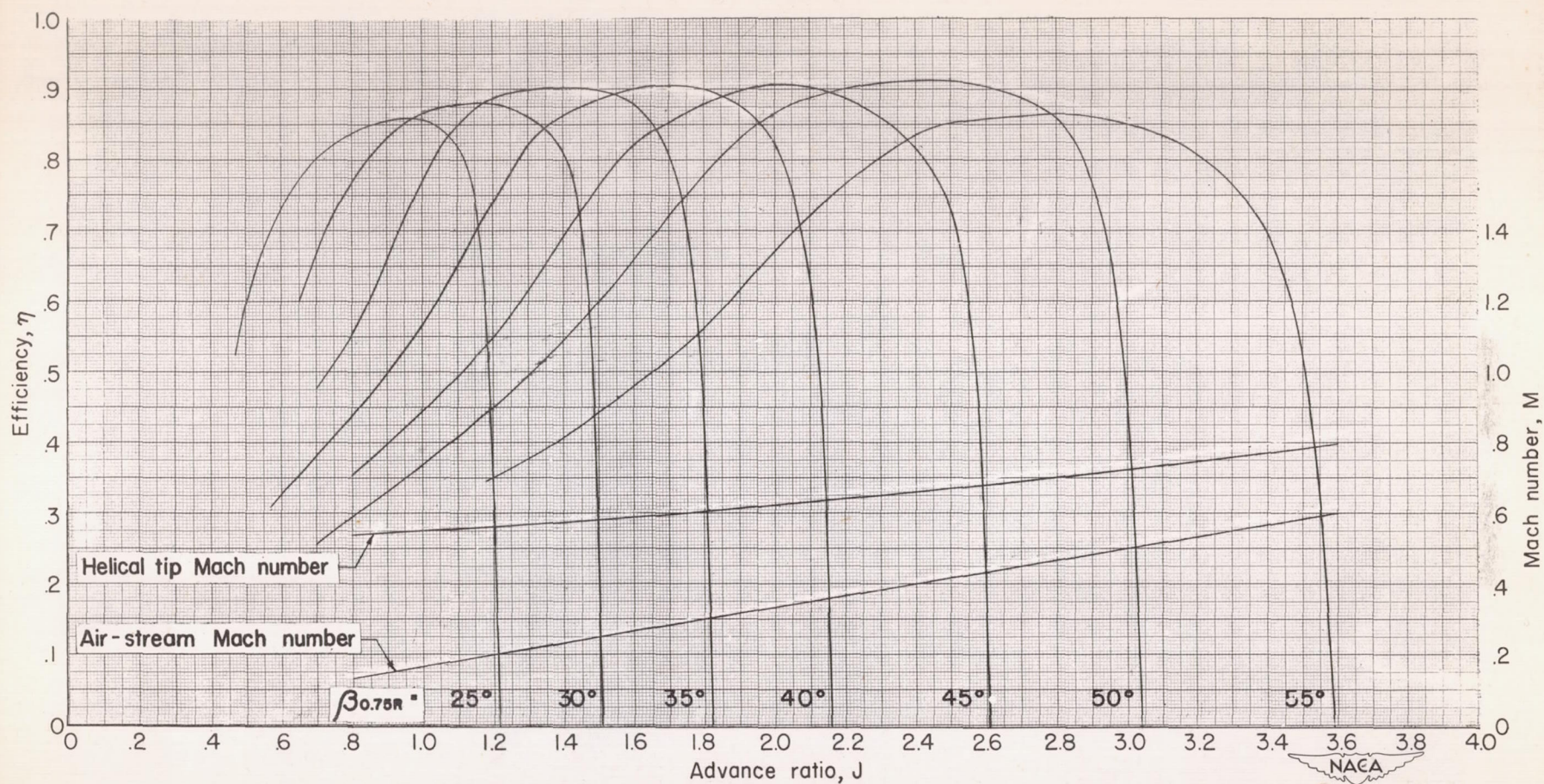
(a) Thrust coefficient.

Figure 2.- Characteristics of NACA 10-(3)(12)-03 propeller at 1140 rpm.



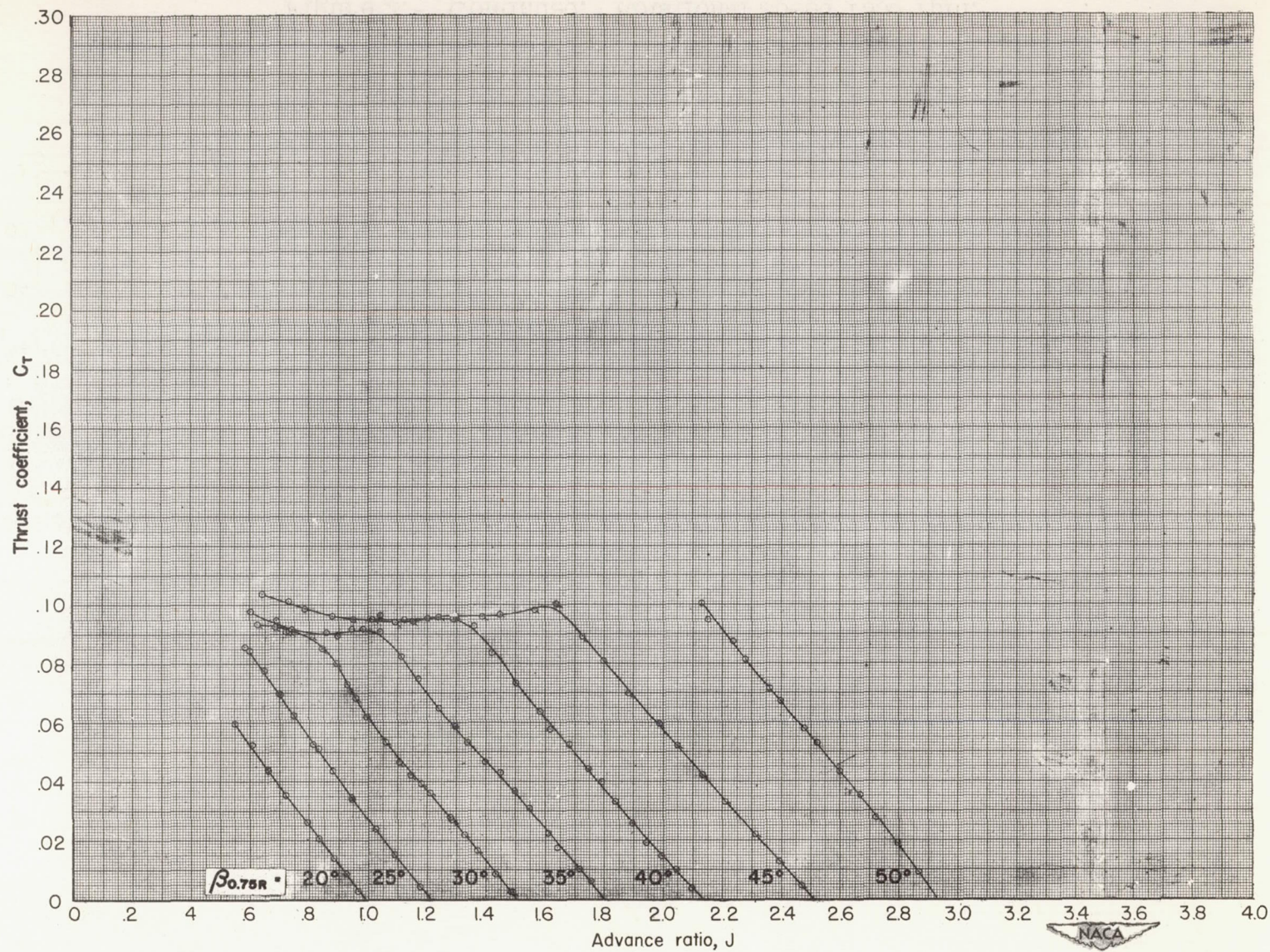
(b) Power coefficient.

Figure 2.- Continued. Rotational speed 1140 rpm.



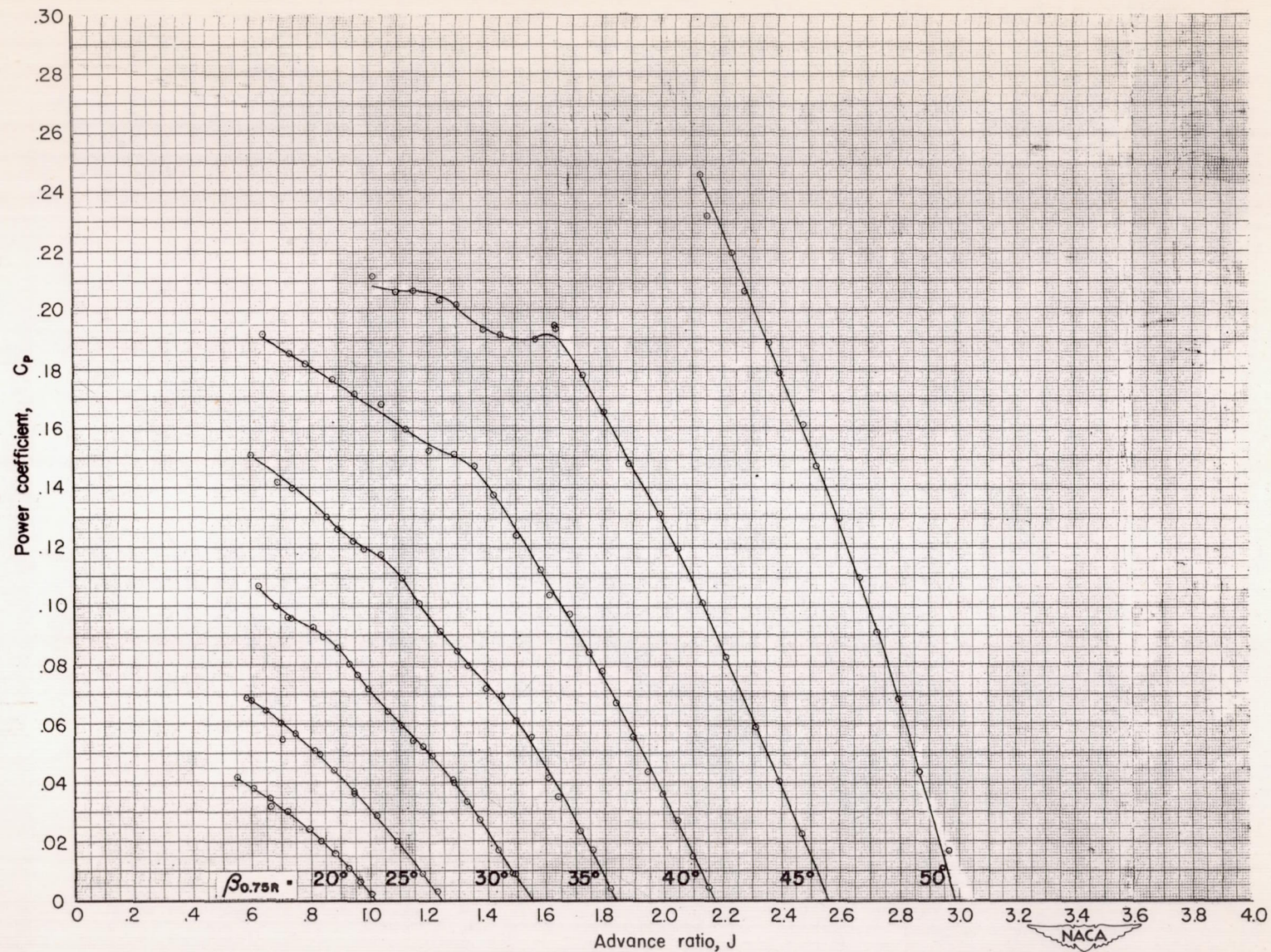
(c) Efficiency.

Figure 2.- Concluded. Rotational speed 1140 rpm.



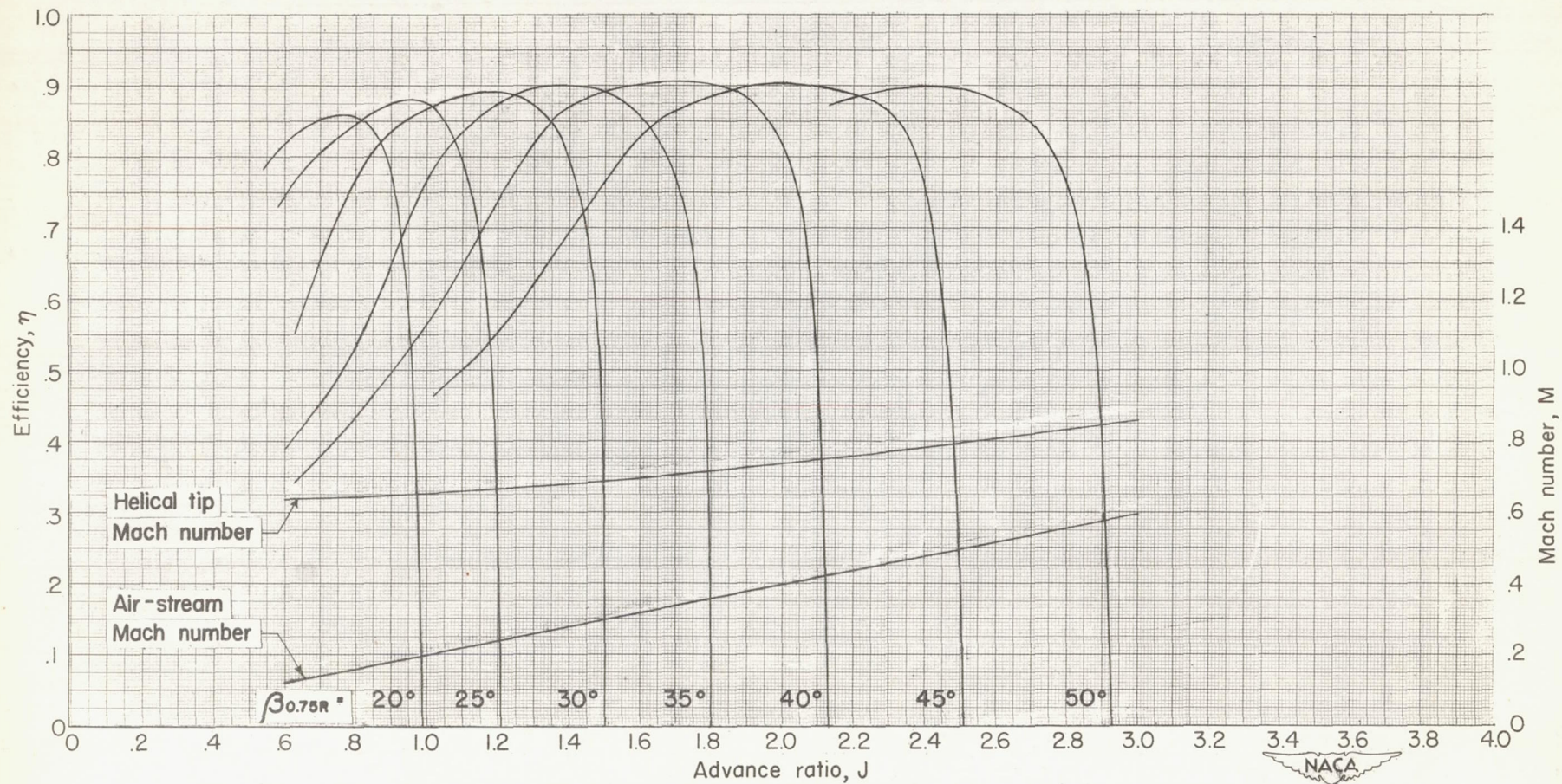
(a) Thrust coefficient.

Figure 3.- Characteristics of NACA 10-(3)(12)-03 propeller at 1350 rpm.



(b) Power coefficient.

Figure 3.- Continued. Rotational speed 1350 rpm.



(c) Efficiency.

Figure 3.- Concluded. Rotational speed 1350 rpm.

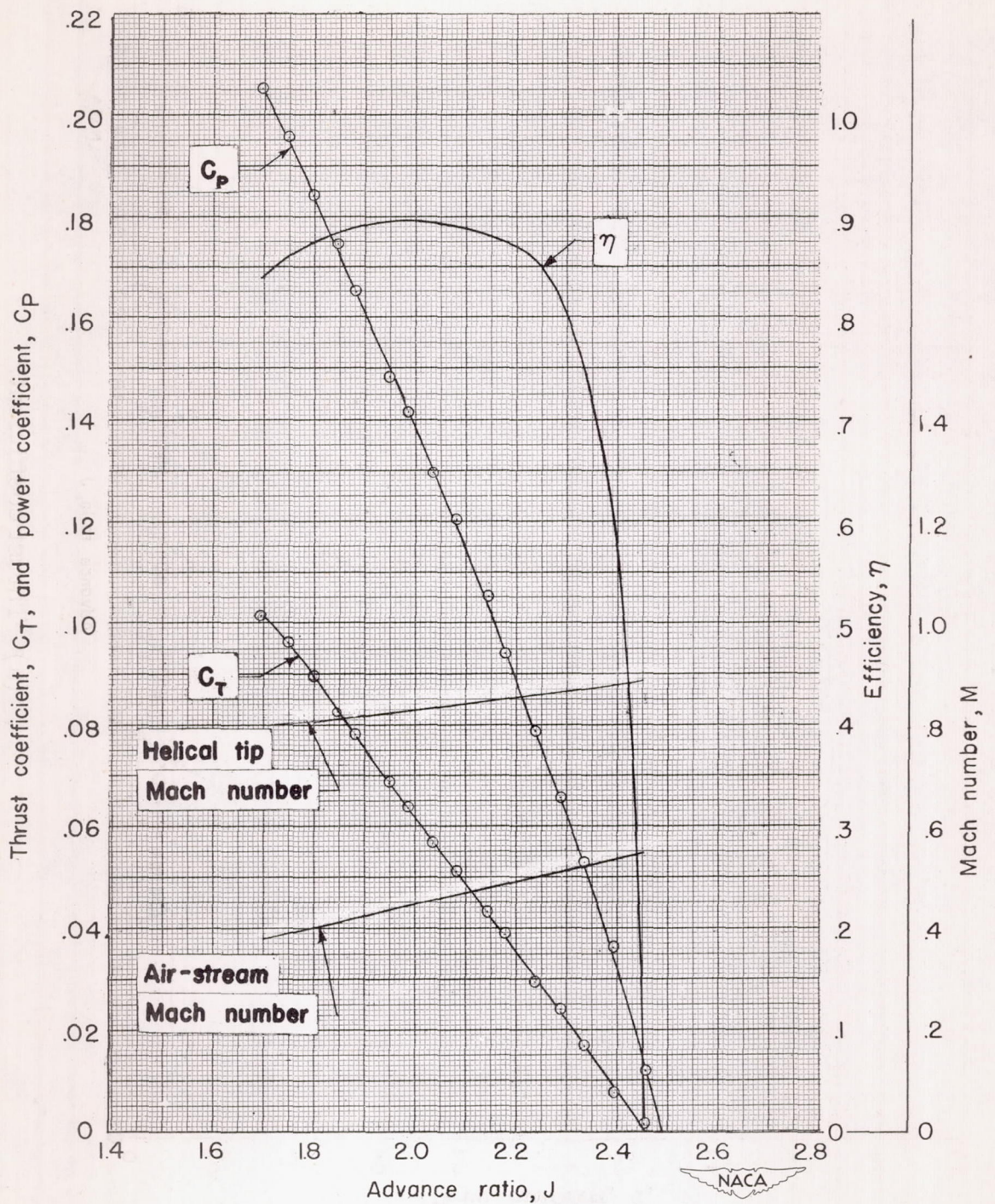
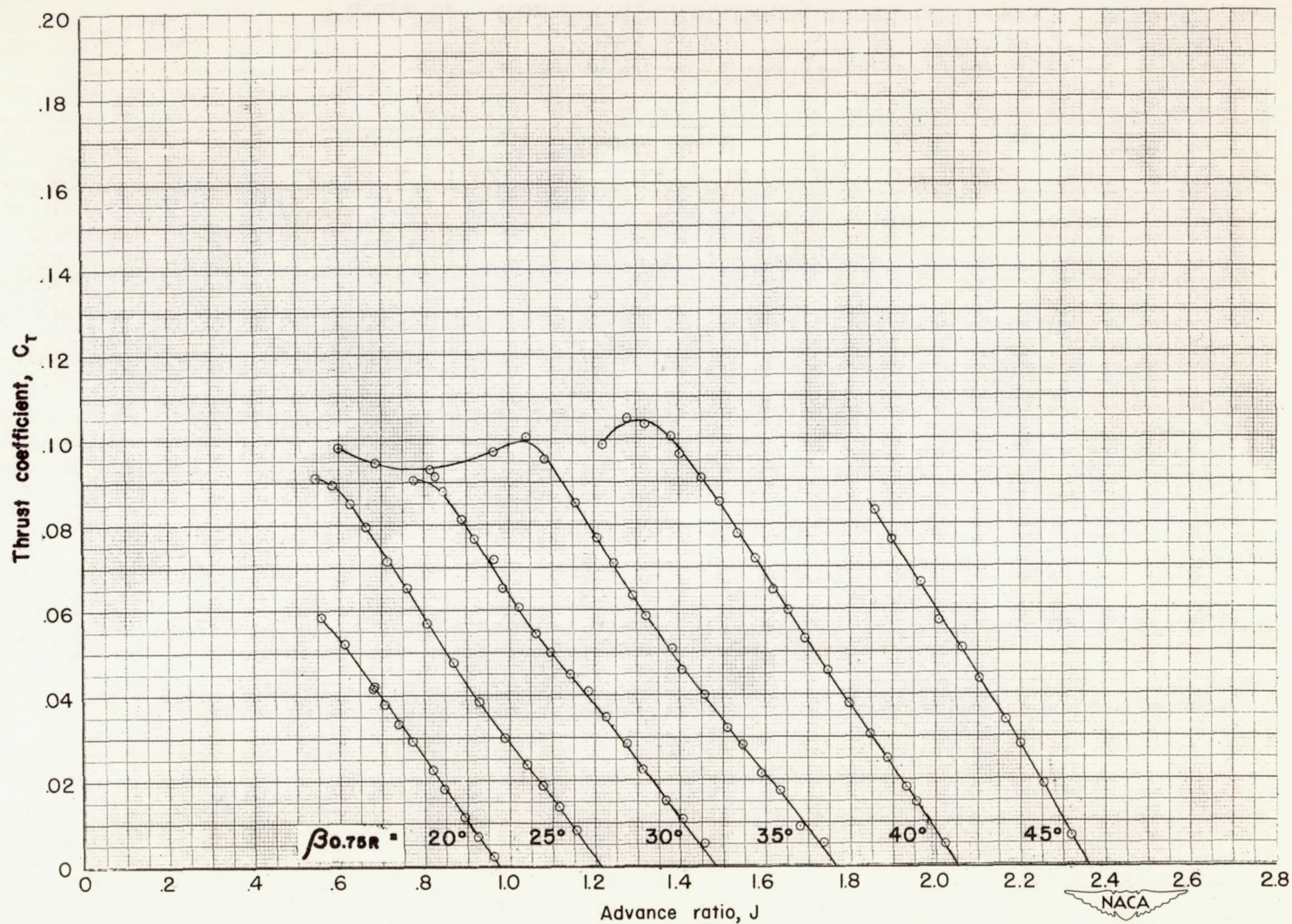
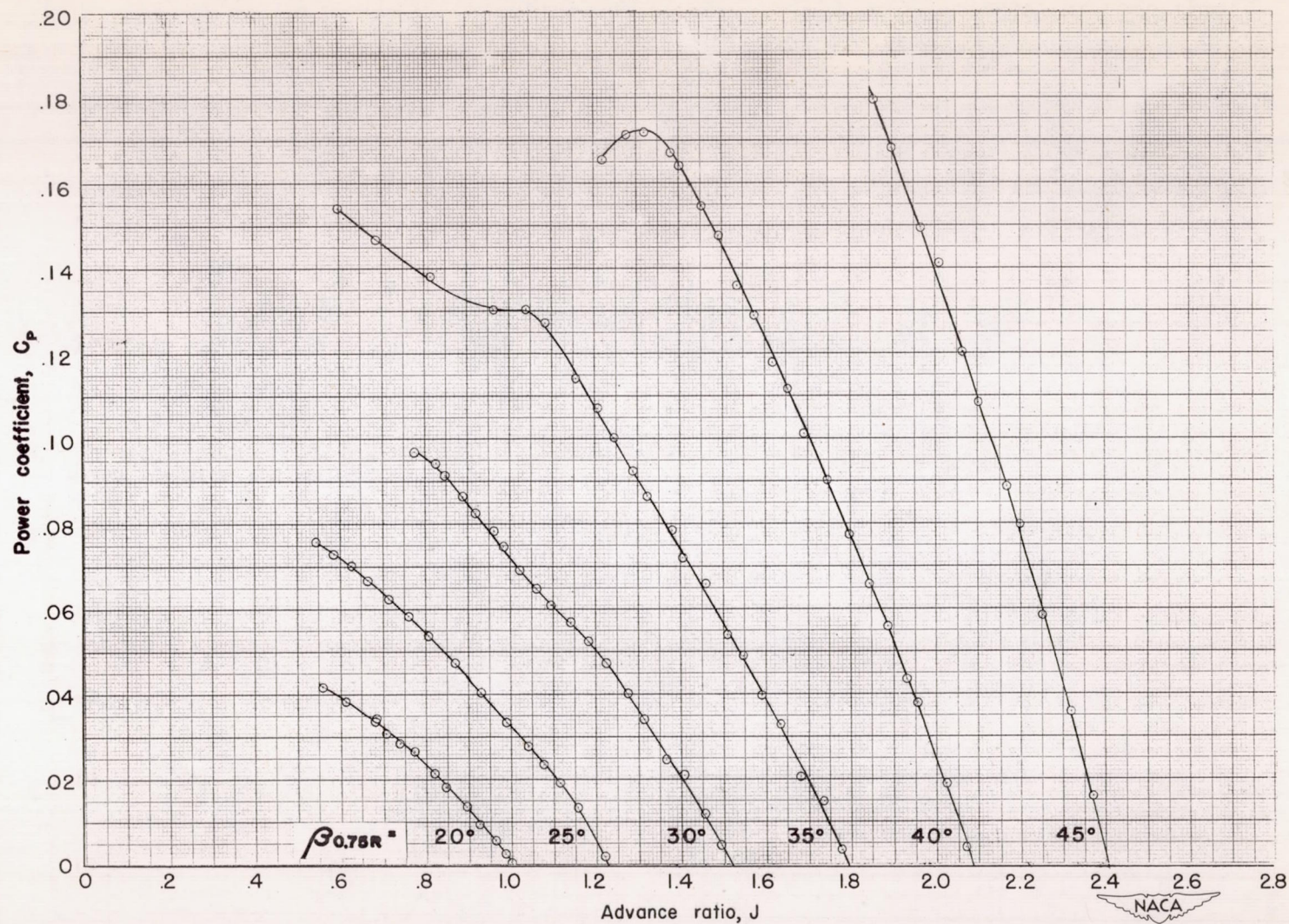


Figure 4.- Characteristics of NACA 10-(3)(12)-03 propeller at 1500 rpm.
 $\beta_{0.75R} = 45^\circ$.



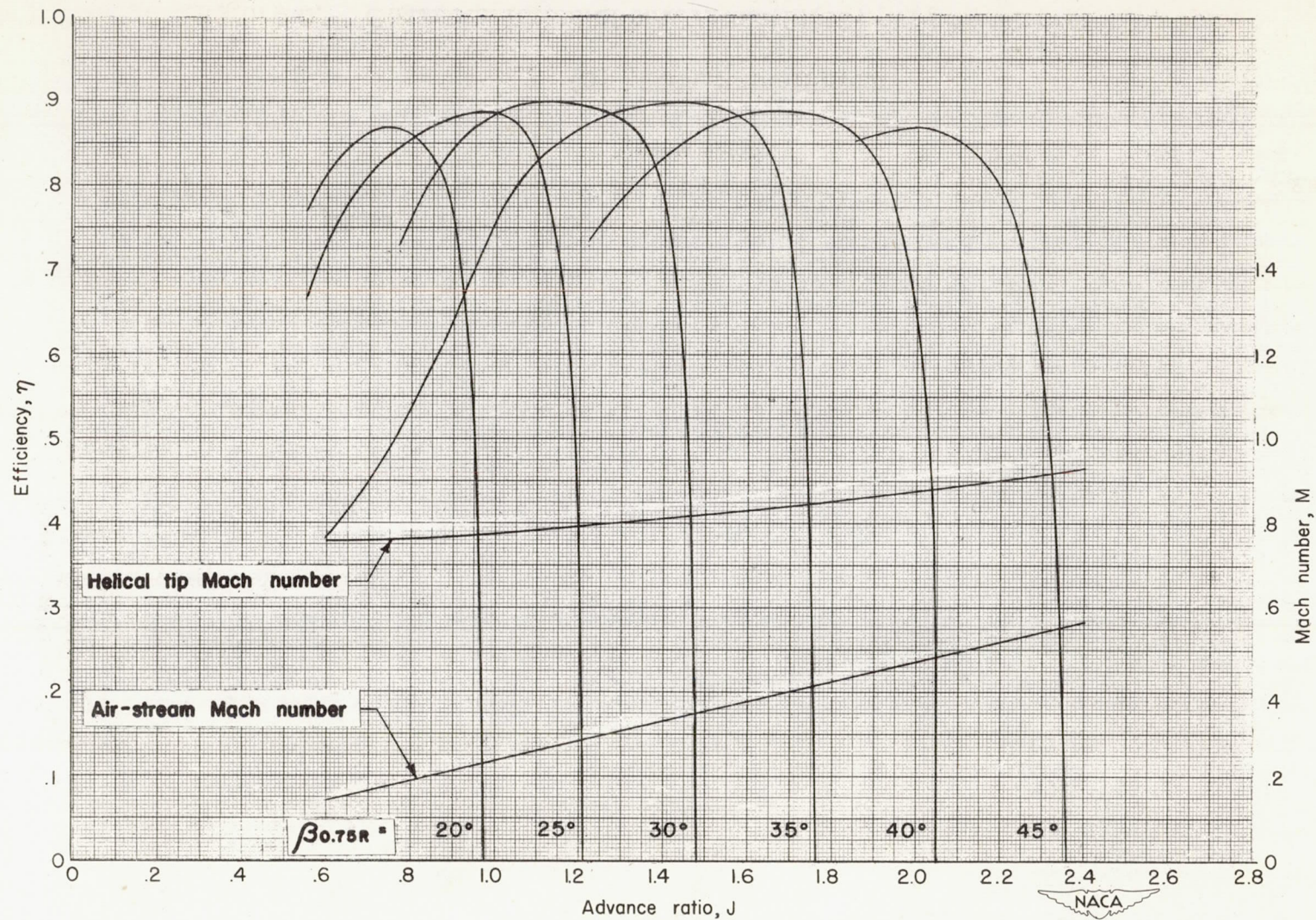
(a) Thrust coefficient.

Figure 5.- Characteristics of NACA 10-(3)(12)-03 propeller at 1600 rpm.



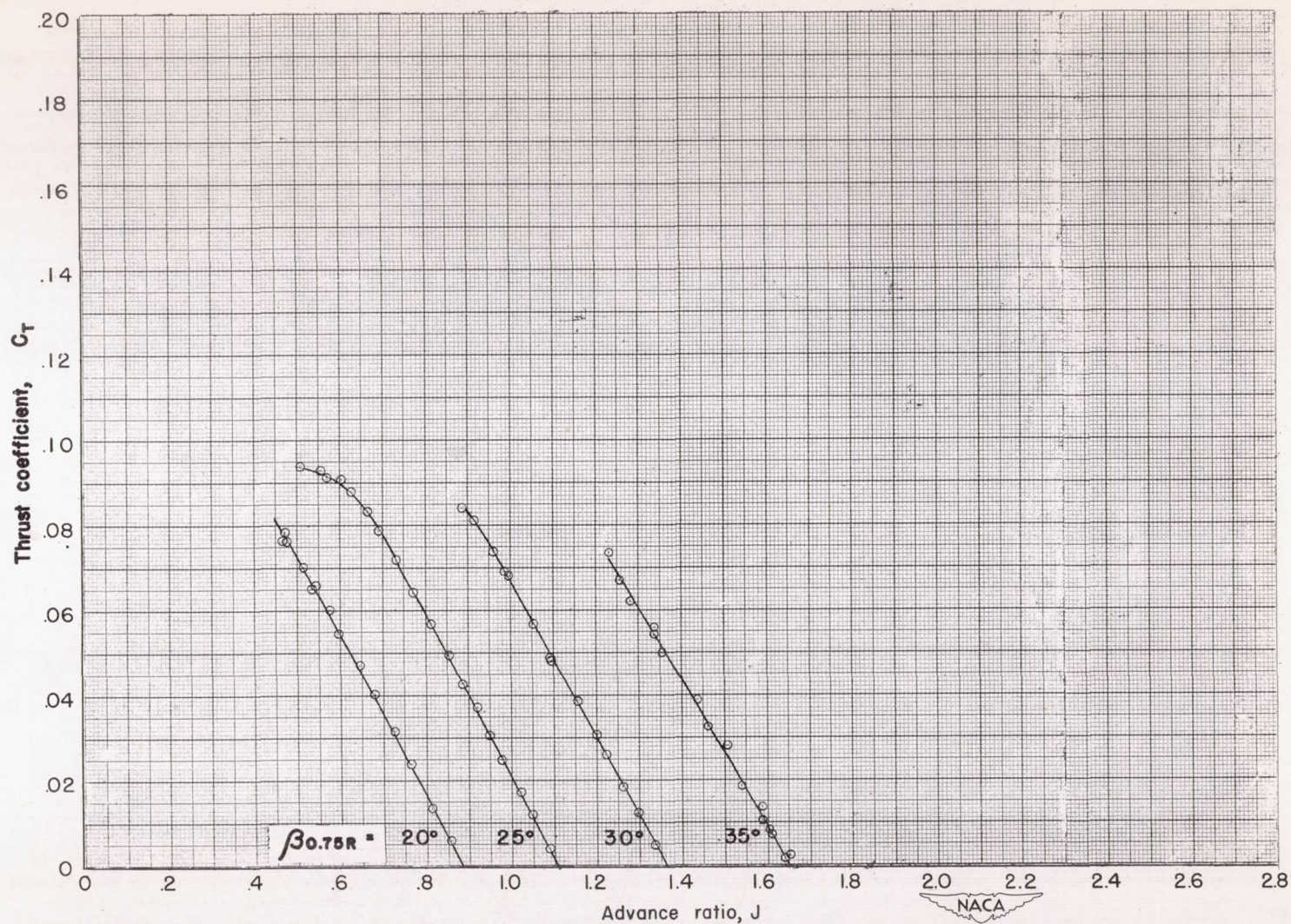
(b) Power coefficient.

Figure 5.- Continued. Rotational speed 1600 rpm.



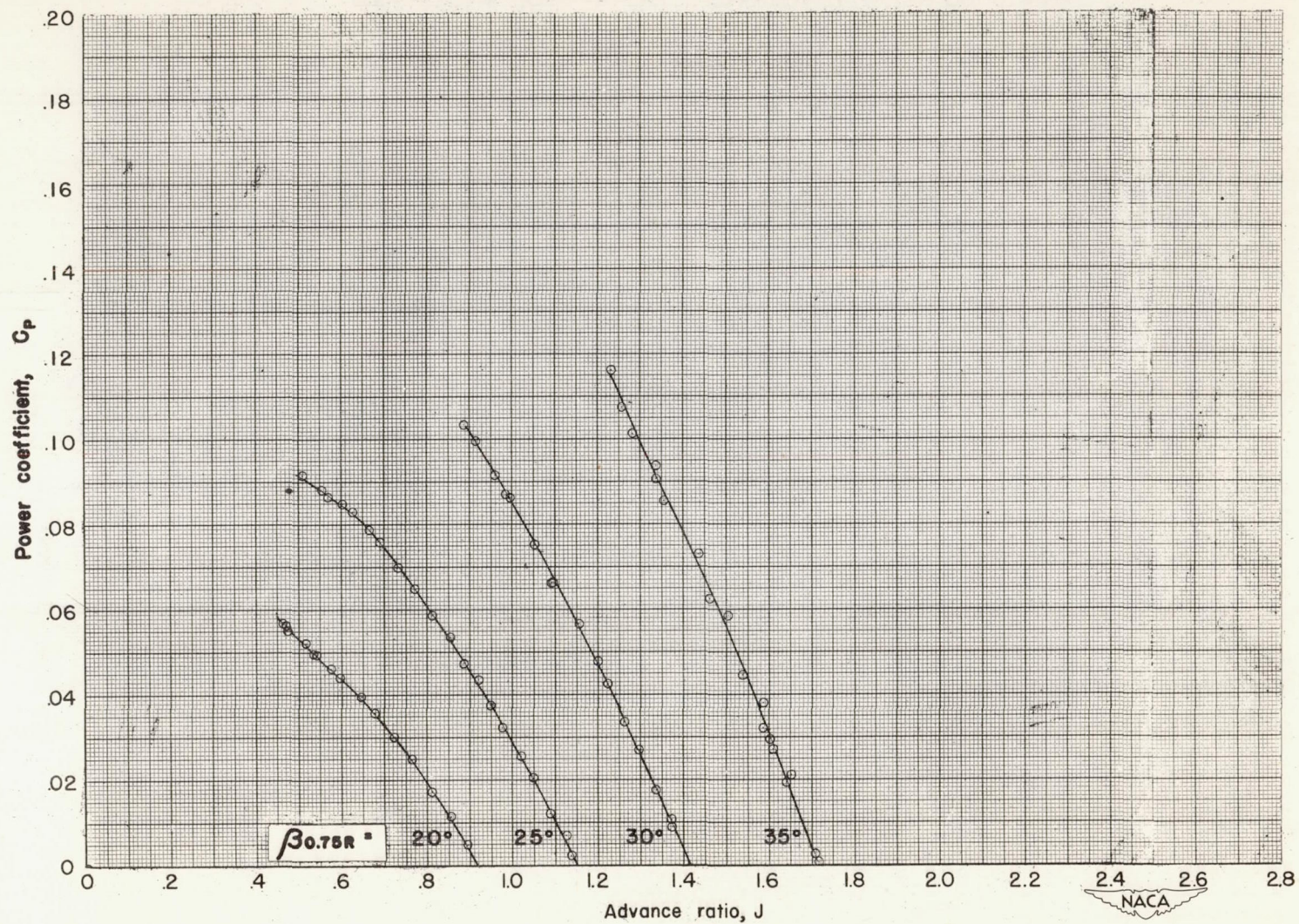
(c) Efficiency.

Figure 5.- Concluded. Rotational speed 1600 rpm.



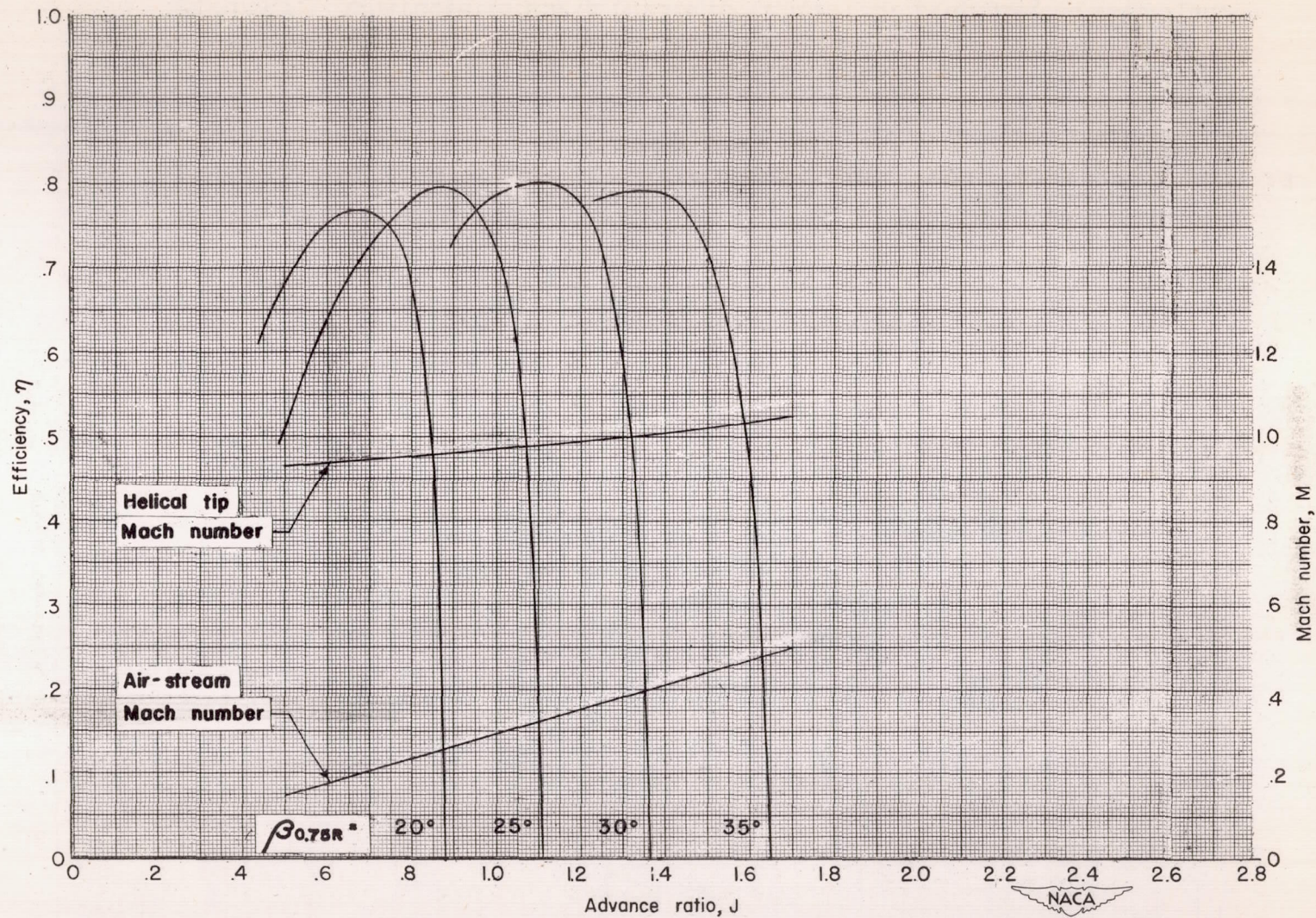
(a) Thrust coefficient.

Figure 6.- Characteristics of NACA 10-(3)(12)-03 propeller at 2000 rpm.



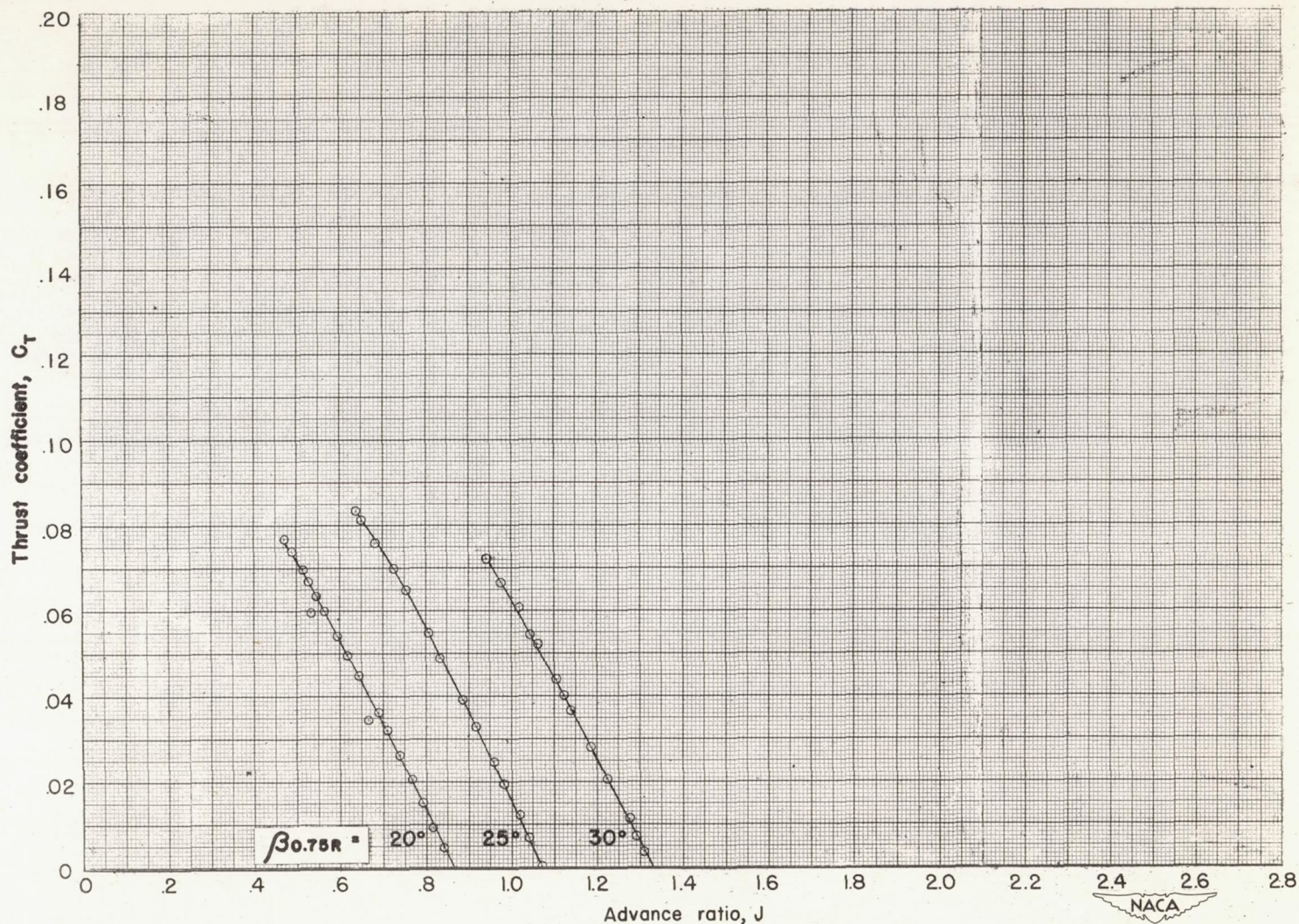
(b) Power coefficient.

Figure 6.- Continued. Rotational speed 2000 rpm.



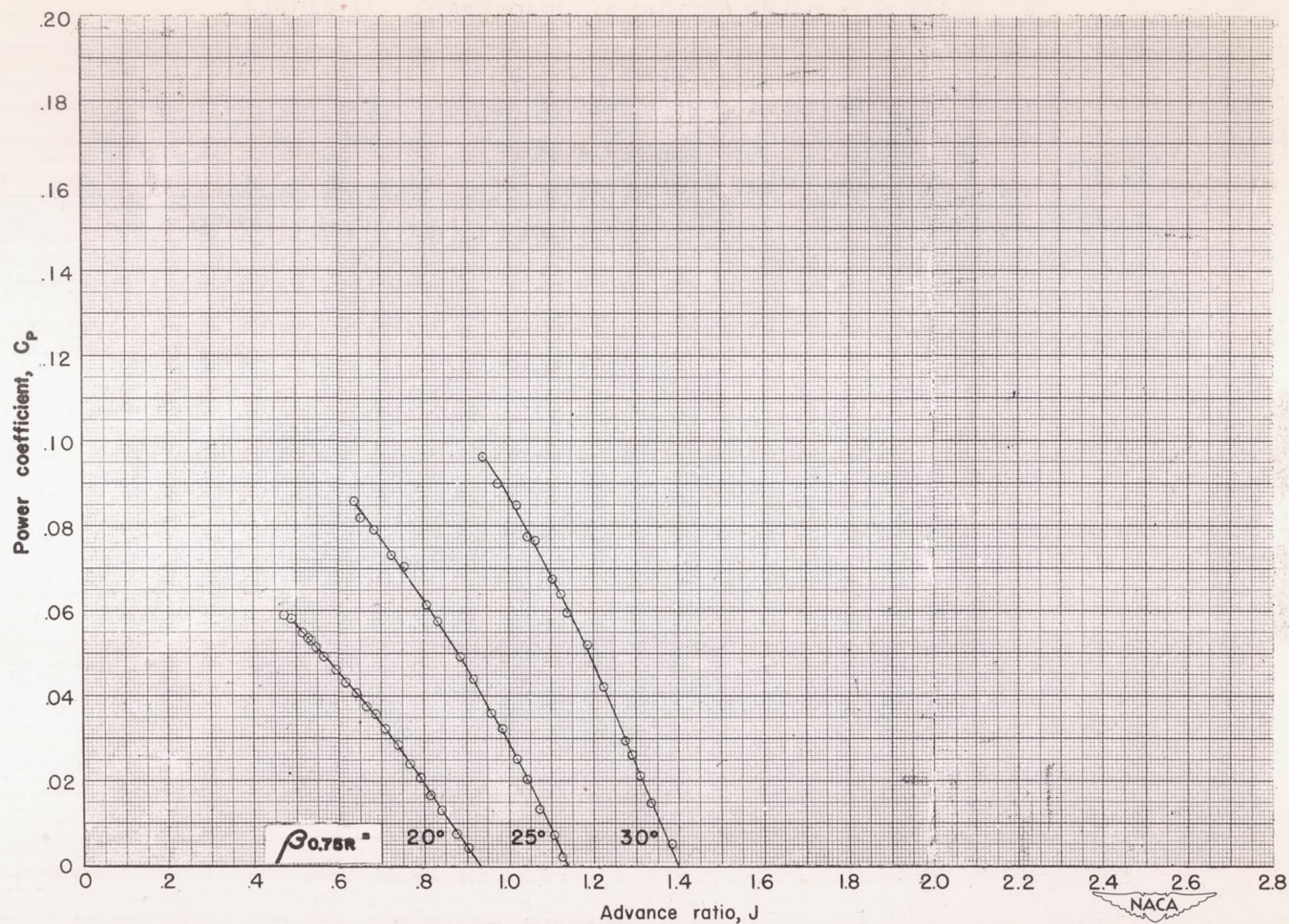
(c) Efficiency.

Figure 6.- Concluded. Rotational speed 2000 rpm.



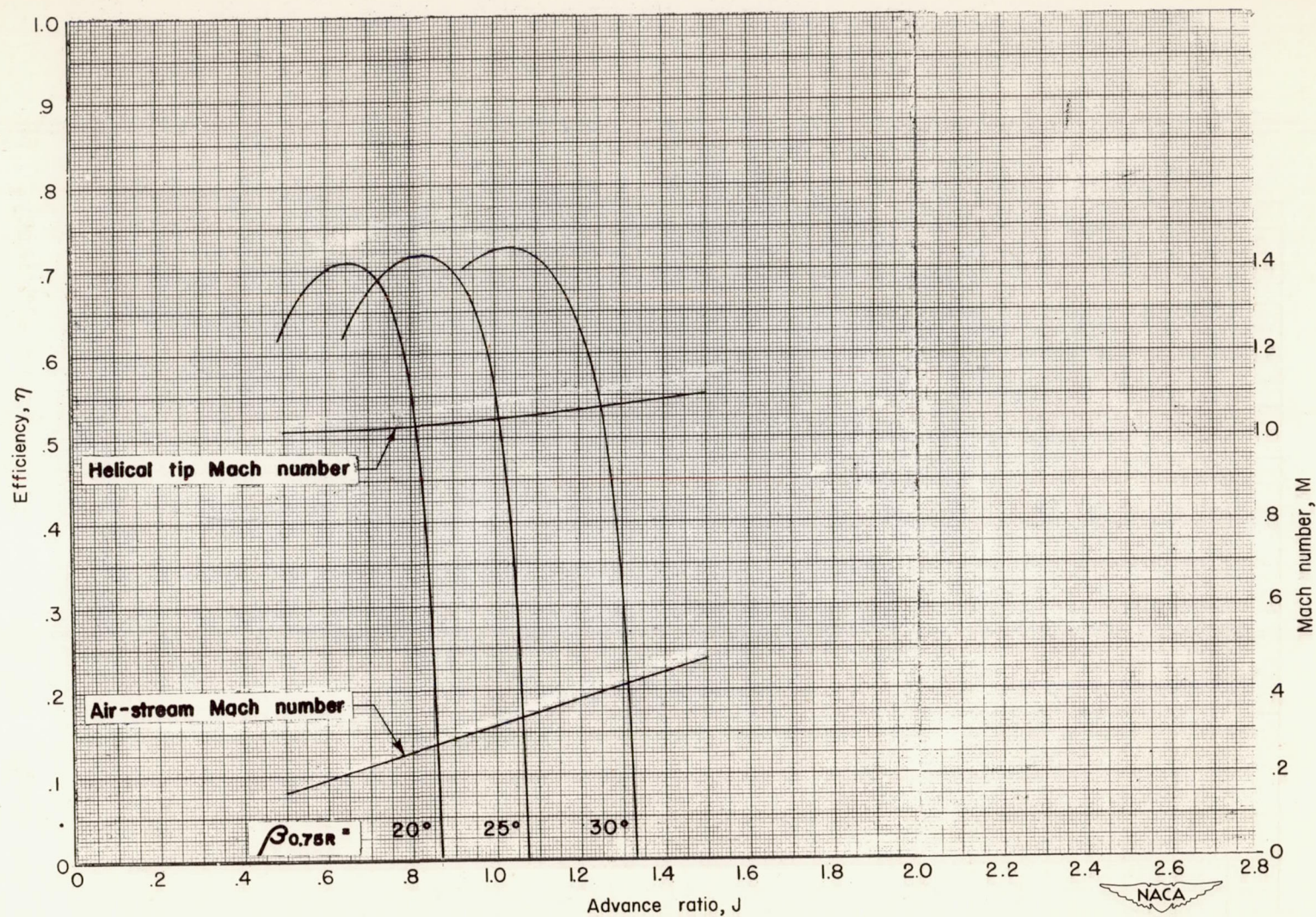
(a) Thrust coefficient.

Figure 7.- Characteristics of NACA 10-(3)(12)-03 propeller at 2160 rpm.



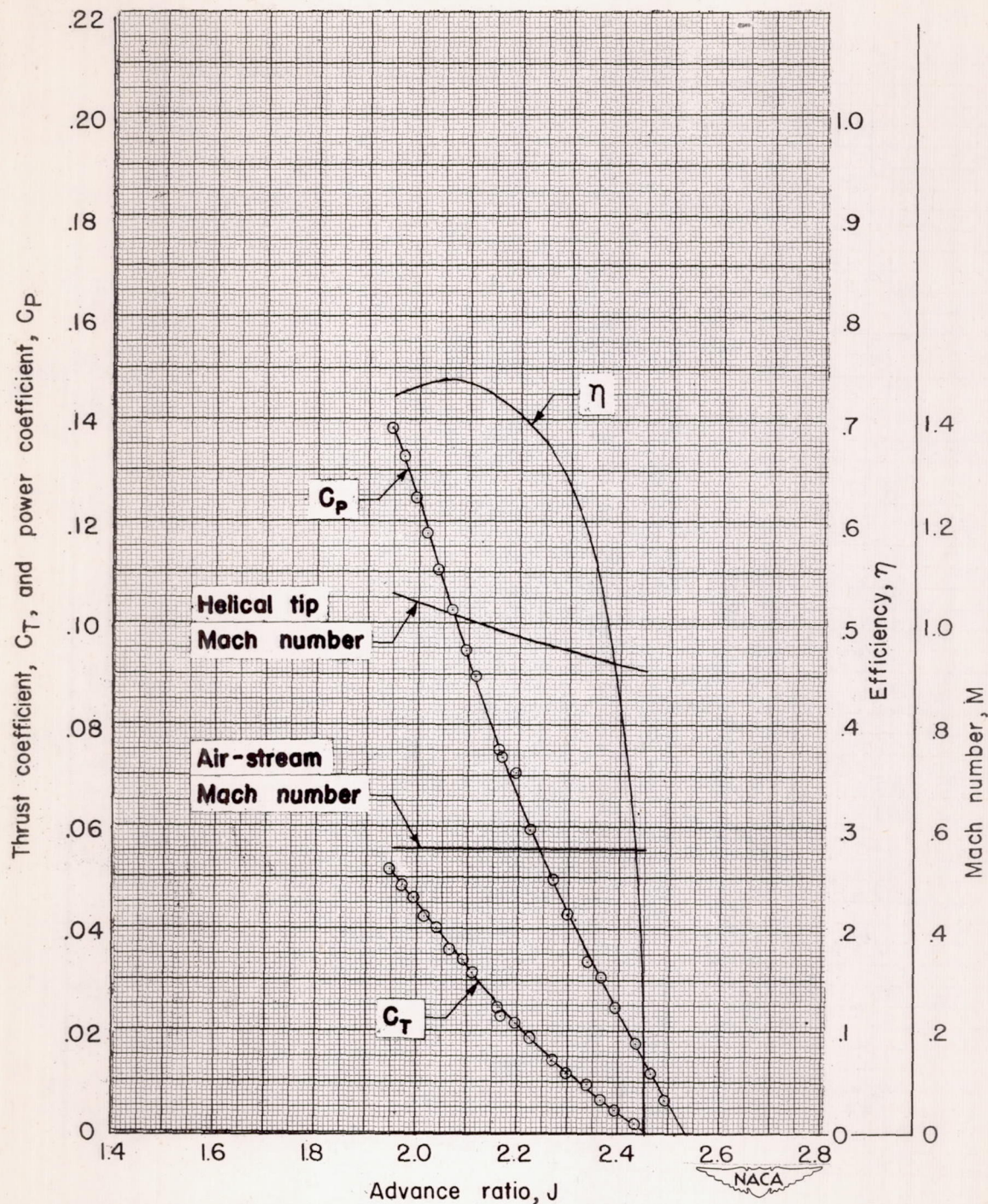
(b) Power coefficient.

Figure 7.- Continued. Rotational speed 2160 rpm.



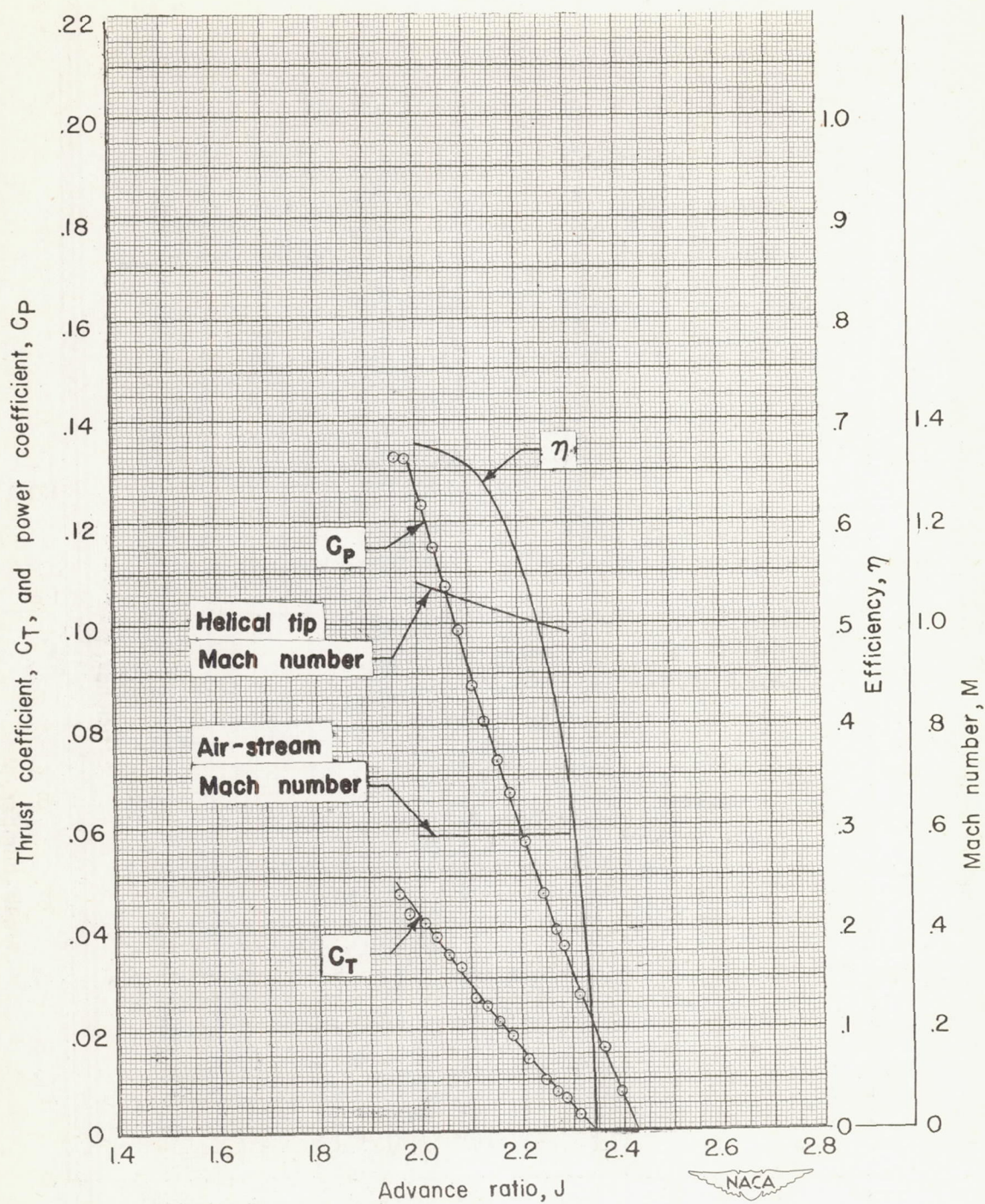
(c) Efficiency.

Figure 7.- Concluded. Rotational speed 2160 rpm.



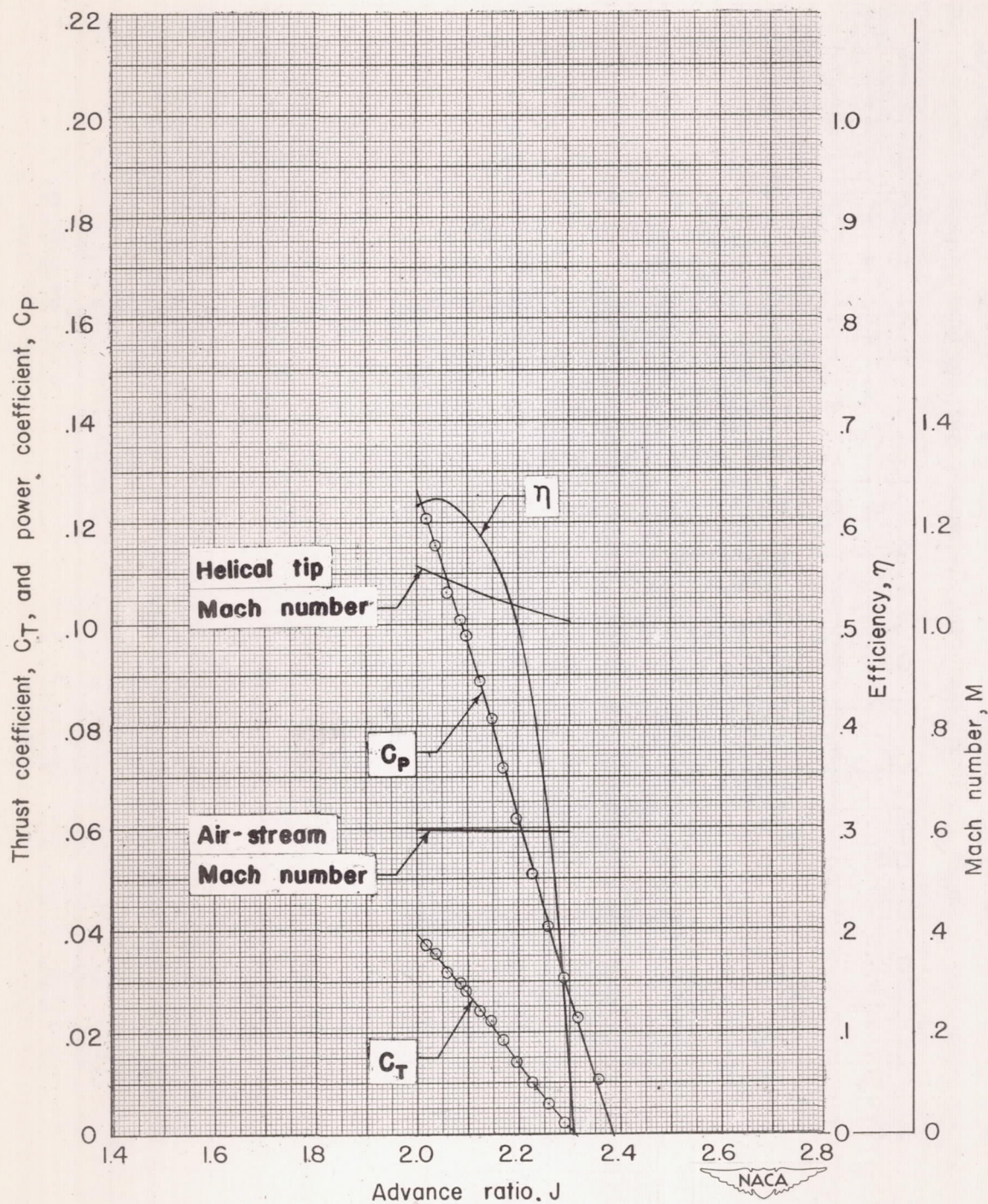
(a) Air-stream Mach number at maximum efficiency, 0.56.

Figure 8.- Characteristics of NACA 10-(3)(12)-03 propeller at high forward speeds. $\beta_{0.75R} = 45^\circ$.



(b) Air-stream Mach number at maximum efficiency, 0.58.

Figure 8.- Continued.



(c) Air-stream Mach number at maximum efficiency, 0.60.

Figure 8.- Concluded.

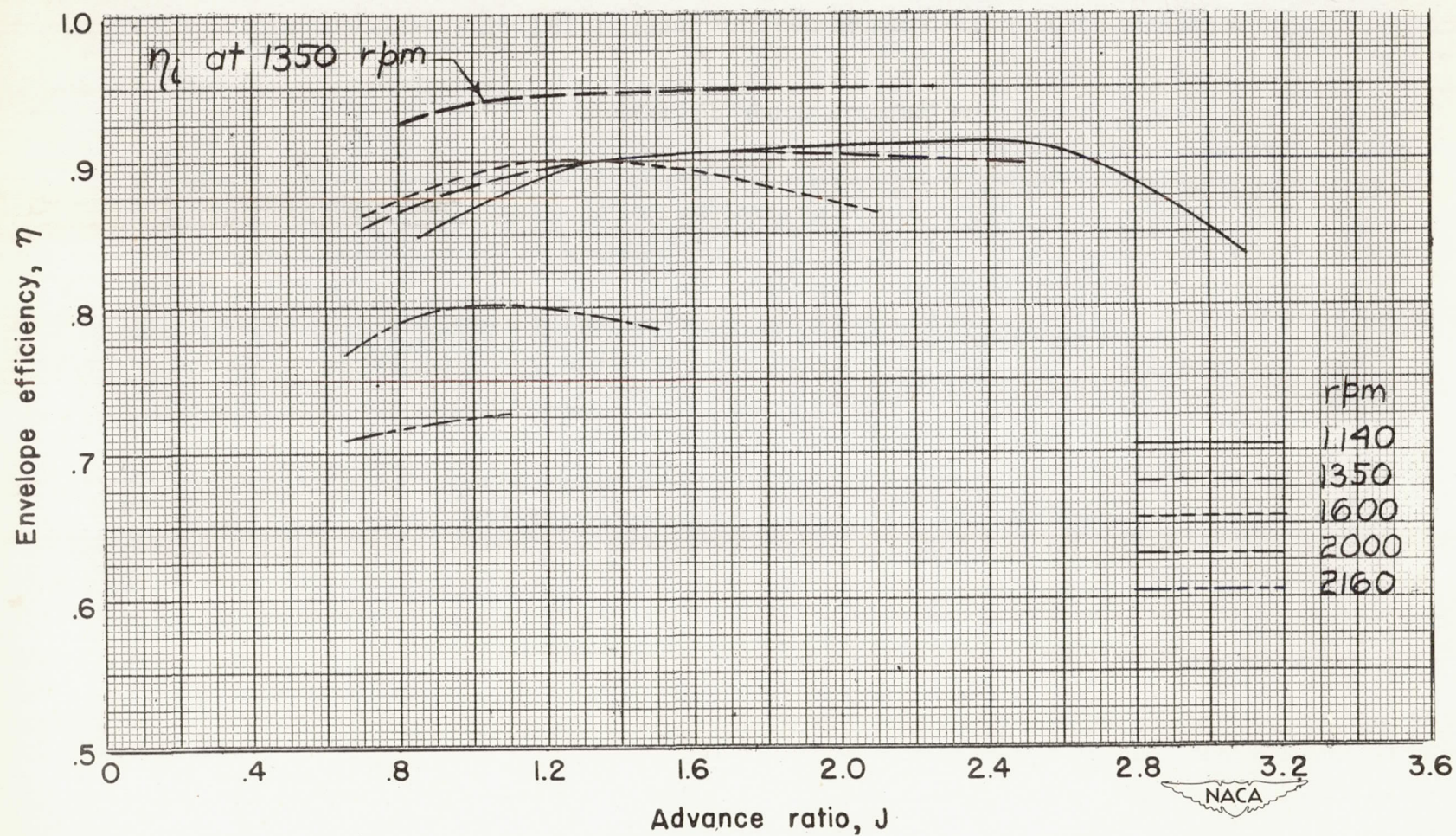


Figure 9.- Envelope efficiency of NACA 10-(3)(12)-03 propeller.

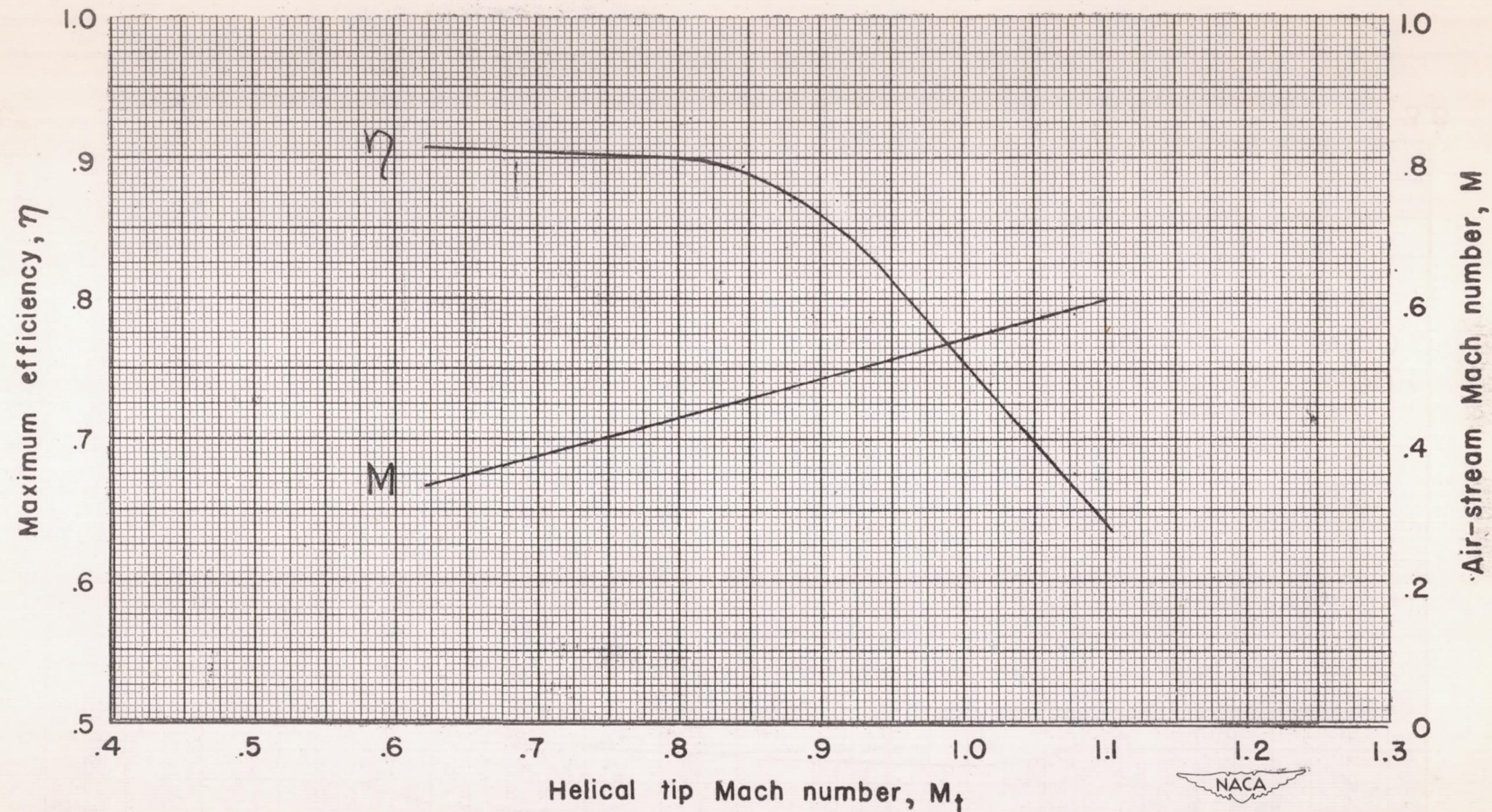


Figure 10.- Effect of tip Mach number on peak efficiency, $\beta_{0.75R} = 45^\circ$.

